Thermoelectric Properties of the New Polytelluride $Ba_3Cu_{14-\delta}Te_{12}$

Abdeljalil Assoud,[†] Stephanie Thomas,[†] Brodie Sutherland,[†] Huqin Zhang,[‡] Terry M. Tritt,[‡] and Holger Kleinke*,[†]

Department of Chemistry, University of Waterloo, Waterloo, Ontario, Canada N2L 3G1, and Department of Physics and Astronomy, Clemson University, Clemson, South Carolina 29634-0978

Received April 3, 2006. Revised Manuscript Received June 5, 2006

$Ba_3Cu_{14-\delta}Te_{12}$ was prepared by directly reacting the elements in stoichiometric ratios at 800 °C for 3 days, followed by slow cooling. $Ba_3Cu_{14-\delta}Te_{12}$ forms a new structure type, space group $P2_1/m$, with lattice dimensions of $a = 11.909(2)$ Å, $b = 21.174(4)$ Å, $c = 11.983(2)$ Å, $\beta = 117.071(4)°$, and $V = 2690.6(8)$ Å^3, for $\delta = 0.35(2)$ ($Z = 4$). The structure contains corner-, edge-, and face-sharing $CuTe_4$ tetrahedra interconnected with almost planar $CuTe_3$ units. These connections result in a three-dimensional Cu atom network with numerous Cu−Cu bonds. With two Te_2^{2-} dumbbells per formula unit, $Ba_3Cu_{14-\delta}Te_{12}$ is an electron-precise compound when $\delta = 0$, according to $(Ba^{2+})_3(Cu^+)_{14}(Te_2^{2-})_2(Te^{2-})_8$. For $\delta > 0$, the materials are degenerate semiconductors with moderate Seebeck coefficients and electrical conductivities, in accord with the electronic structure calculations, and exhibit extremely low thermal conductivity.

Introduction

Thermoelectric materials are utilized to convert a temperature gradient (e.g., from waste heat) into electricity or to convert electricity into a temperature gradient (e.g., for cooling).[1,2] Ideally, a thermoelectric material exhibits a high Seebeck coefficient, high electrical conductivity, and low thermal conductivitiy. The best thermoelectrics are small gap semiconductors comprising heavy elements,[2,3] with gaps between 6 and 10 k_BT, with k_B = Boltzmann constant and T = operating temperature, hence 0.16−0.26 eV at room temperature.[4] Recent success from various research groups[5−9] reinforces the expectation to find more efficient materials soon. With many of the best materials known to date being main group tellurides, we have explored new ternary tin chalcogenides (e.g., the mixed valent $SrSn_2Se_4$[10] and the polychalcogenides Sr_2SnSe_5, Ba_2SnSe_5,[11] and Ba_2SnTe_5[12]) as well as quaternary copper tin chalcogenides ($BaCu_2SnSe_4$ and $Ba_3Cu_2Sn_3Se_{10}$[13]). These materials exhibit band gaps starting from 0.2 eV, and rather high Seebeck coefficients, but low electrical conductivities. Despite earlier investigations, manifested in reports from the year 2001 on the thermoelectric properties of $BaCu_2Te_2$[14] and $A_2BaCu_8Te_{10}$ (A = K, Rb, Cs),[15] we were able to discover a new ternary barium copper telluride, namely, $Ba_3Cu_{14-\delta}Te_{12}$. With this contribution, the synthesis and structure of this material, together with its thermoelectric properties, are presented.

Experimental Section

Synthesis. The reactions were started from the elements (Ba: 99% nominal purity, pieces, Aldrich; Cu: 99.5%, powder −150 mesh; ALFA AESAR; Te: 99.8%, powder −200 mesh, Aldrich), with sample masses of approximately 1 g. The elements were stored and handled in a glovebox filled with argon. In that glovebox, the elements were placed into fused silica tubes, which were then sealed under vacuum (10^{-2} mbar). Initially, $Ba_3Cu_{14-\delta}Te_{12}$ was found in a reaction starting from the elements in the ratio of Ba:Cu:Te = 1:6:5, the intention being to find a new Cu-rich polytelluride. The mixture was heated to 800°C, held at that temperature for 4 days, and then cooled to room temperature within 8 days (reaction I). After solving the crystal structure using a single crystal of this reaction (crystal I), the formula was identified as $Ba_3Cu_{13.43(5)}Te_{12}$. In a subsequent reaction, reaction II, a mixture of 3:14:12 Ba:Cu:Te was heated to 800 °C within 48 h, held at 800 °C for 100 h, and then cooled to room temperature within 200 h. From that reaction a higher quality crystal (crystal II) was chosen to determine the structure with higher accuracy (see Structure Determination) and to check for the existence of a phase range.

Phase-pure samples of $Ba_3Cu_{14-\delta}Te_{12}$, as analyzed via X-ray powder diffraction utilizing the INEL powder diffractometer with

* To whom correspondence should be addressed. E-mail: kleinke@uwaterloo.ca.
† University of Waterloo.
‡ Clemson University.

(1) Tritt, T. M. *Science* **1999**, *283*, 804−805.
(2) DiSalvo, F. J. *Science* **1999**, *285*, 703−706.
(3) Rowe, D. M. *CRC Handbook of Thermoelectrics*; CRC Press: Boca Raton, FL, 1995.
(4) Sofo, J. O.; Mahan, G. D. *Phys. Rev. B* **1994**, *49*, 4565−4570.
(5) Sales, B. C.; Mandrus, D.; Williams, R. K. *Science* **1996**, *272*, 1325−1328.
(6) Chung, D.-Y.; Hogan, T.; Brazis, P.; Rocci-Lane, M.; Kannewurf, C.; Bastea, M.; Uher, C.; Kanatzidis, M. G. *Science* **2000**, *287*, 1024−1027.
(7) Venkatasubramanian, R.; Slivola, E.; Colpitts, T.; O'Quinn, B. *Nature* **2001**, *413*, 597−602.
(8) Hsu, K. F.; Loo, S.; Guo, F.; Chen, W.; Dyck, J. S.; Uher, C.; Hogan, T.; Polychroniadis, E. K.; Kanatzidis, M. G. *Science* **2004**, *303*, 818−821.
(9) Chung, D.-Y.; Hogan, T. P.; Rocci-Lane, M.; Brazis, P.; Ireland, J. R.; Kannewurf, C. R.; Bastea, M.; Uher, C.; Kanatzidis, M. G. *J. Am. Chem. Soc.* **2004**, *126*, 6414−6428.
(10) Assoud, A.; Soheilnia, N.; Kleinke, H. *Chem. Mater.* **2004**, *16*, 2215−2221.
(11) Assoud, A.; Soheilnia, N.; Kleinke, H. *J. Solid State Chem.* **2005**, *178*, 1087−1093.
(12) Assoud, A.; Derakhshan, S.; Soheilnia, N.; Kleinke, H. *Chem. Mater.* **2004**, *16*, 4193−4198.
(13) Assoud, A.; Soheilnia, N.; Kleinke, H. *Chem. Mater.* **2005**, *17*, 2255−2261.
(14) Wang, Y. C.; DiSalvo, F. J. *J. Solid State Chem.* **2001**, *156*, 44−50.
(15) Patschke, R.; Zhang, X.; Singh, D.; Schindler, J.; Kannewurf, C. R.; Lowhorn, N.; Tritt, T.; Nolas, G. S.; Kanatzidis, M. G. *Chem. Mater.* **2001**, *13*, 613−621.

10.1021/cm060776k CCC: $33.50
Published on Web 07/01/2006

a position-sensitive detector, were obtained for $0.025 < \delta < 0.875$ by melting the corresponding mixtures at 800 °C for 2 h, followed by annealing at 600 °C over a period of 2 weeks (336 h). These reactions were finished by switching off the resistance furnace.

Analysis. An EDX investigation (EDX: energy dispersive analysis of X-rays) using an electron microscope (LEO 1530) with an additional EDX device (EDAX Pegasus 1200) was performed on selected $Ba_3Cu_{14-\delta}Te_{12}$ crystals with $\delta = 0.025$ and 0.75. The scans were performed with an acceleration voltage of 21 kV under high dynamic vacuum. No impurities (e.g., stemming from the reaction container) were detected. Taking the Kα peak of Cu (at 8.060 keV) and the Lα peaks of Ba and Te (at 4.465 and 3.769 keV, respectively) into account for the (standardless) quantitative analysis, the Ba:Cu:Te ratios were calculated to be (averaged over four crystals) 10.5:46.3:43.2 at. % for $\delta = 0.025$ and 10.5:45.1:44.4 at. % for $\delta = 0.75$. For comparison, the expected values are 10.4:48.2:41.4 at. % for $\delta = 0.025$ and 10.6:46.9:42.5 at. % for $\delta = 0.75$.

Structure Determination. Two X-ray single-crystal structure studies were performed on single crystals selected from reactions I and II, respectively. A BRUKER Smart APEX CCD diffractometer with graphite-monochromatized Mo $K\alpha_1$ radiation was used for the data collection, performed by scans of 0.3° in ω in two groups of 606 frames (each with an exposure time of 60 s) at $\phi =$ 0° and 60°. The data were corrected for Lorentz and polarization effects. Absorption corrections were based on fitting a function to the empirical transmission surface as sampled by multiple equivalent measurements using SADABS.[16]

The structure solution and refinements were carried out with the SHELXTL program package.[17] The lattice parameters pointed toward monoclinic symmetry, later confirmed by good internal R values (e.g., 4% for $Ba_3Cu_{13.65(2)}Te_{12}$). The systematic absences ($0k0$ absent for all odd k) restricted the space group selection to $P2_1$ and $P2_1/m$. Refinements were successful in both space groups and did not differ significantly, aside from strong correlation factors in $P2_1$. Hence, the centrosymmetric space group was chosen, in accord with the E_{hkl} statistics. SHELXS ("Direct Methods") found 18 atomic sites in the case of the first structure analysis (crystal from reaction I), to which Ba and Te atoms were readily assigned. Eighteen Cu atom sites were detected in the difference Fourier map. Subsequent refinements against F^2 converged to reasonable residual values, e.g., $R_w(F_o^2) = 0.140$. Then the atomic positions were standardized using the program TIDY within the PLATON package.[18] The highest peak of the difference Fourier map (11.6 $e^-/Å^3$) was surrounded by four Te sites in distances >2.5 Å, typical for a Cu site. Therefore, this site was refined as a Cu-deficient site (Cu19). Last, because the Cu sites exhibited a large range of equivalent displacement parameters, i.e., between 0.173(5) and 0.099(1) $Å^2$, the occupancy of each Cu site was refined separately. Toward this end, all those Cu sites were treated as fully occupied, which exhibited refined occupancies >96%. This resulted in 6 of the 19 Cu sites being significantly deficient, with occupancies between 15% and 92%, and significantly improved R values (e.g., $R_w(F_o^2) = 0.111$). The refined formula was $Ba_3Cu_{13.43(5)}Te_{12}$.

Because of the in part anisotropic and high expansion parameters of the first data collection (crystal I), the second was carried out at 180 K, instead of at room temperature. The refinements with the data from the crystal of reaction II commenced with the final refinement of crystal I described above. Additionally, we again checked for deficiencies on all Cu sites. The deficient Cu sites exhibit occupancies between 4% and 94%, leading to a refined formula of $Ba_3Cu_{13.65(2)}Te_{12}$ (with $R_w(F_o^2) = 0.088$). Other than smaller expansion and unit cell parameters, no obvious temperature effect was noticeable. The unit cell volume decreased by 0.5%, the a and b axes both by 0.2%, and the c axis by 0.04%. To verify whether this is exclusively an effect of the different measurement temperatures, we determined the lattice parameter of a third crystal at both temperatures using the same technique with the Smart APEX CCD. Its unit cell volume shrunk upon cooling slightly more than 0.5%, namely, by 0.6%, from 2710.6(4) to 2695.0(4) $Å^3$. This indicates that the higher Cu content of crystal II leads to a larger unit cell, which was masked by determining the cell at a lower temperature. The crystallographic data are summarized in Table 1 and the atomic parameters including the occupancy factors in Table 2.

Table 1. Crystallographic Data for $Ba_3Cu_{14-\delta}Te_{12}$

refined formula	$Ba_3Cu_{13.65(2)}Te_{12}$	$Ba_3Cu_{13.43(5)}Te_{12}$
formula weight [g/mol]	2810.54	2796.56
T of measurement [K]	180(2)	298(2)
λ [Å]	0.71073	0.71073
space group	$P2_1/m$	$P2_1/m$
a [Å]	11.909(2)	11.9343(7)
b [Å]	21.174(4)	21.222(1)
c [Å]	11.983(2)	11.9882(7)
β [deg]	117.071(4)	117.077(1)
V [$Å^3$]	2690.6(8)	2703.5(3)
Z	4	4
μ [mm^{-1}]	27.589	27.289
ρ_{calcd} [g/cm^3]	6.938	6.871
$R(F_o)^a/R_w(F_o^2)^b$	0.045/0.088	0.051/0.111

[a] $R(F_o) = \Sigma||F_o| - |F_c||/\Sigma|F_o|$. [b] $R_w(F_o^2) = [\Sigma[w(F_o^2 - F_c^2)^2]/\Sigma[w(F_o^2)^2]]^{1/2}$.

Calculation of the Electronic Structure. The LMTO method (LMTO = linear muffin tin orbitals) was employed with atomic spheres approximation (ASA)[19,20] for the electronic structure calculations. In the LMTO approach, the density functional theory is used with the local density approximation (LDA) to treat correlation effects.[21] The following wave functions were used: for Ba 6s, 6p (downfolded[22]), 5d, and 4f; for Cu 4s, 4p, and 3d, and for Te 5s, 5p, and 5d and 4f (the latter two downfolded). All Cu atoms of $Ba_3Cu_{13.65}Te_{12}$ with refined occupancy factors above 90% were treated as fully occupied, the Cu19 site (refined occupancy of 4%) was removed, and two of the four Cu5 positions per cell were filled, resulting in a symmetry reduction to Pm and a formula of $Ba_3Cu_{14}Te_{12}$. The integrations in k space were performed by an improved tetrahedron method[23] on 108 independent k points of a grid of 144 k points evenly spread throughout the first Brillouin zone. The Crystal Orbital Hamilton Population (COHP) curves,[24] together with the integrated COHP values (ICOHPs),[25] were used to extract information about the bond strengths of selected Cu−Cu and Te−Te interactions.

Physical Property Measurements. Cold-pressed bars of the dimensions $6 \times 1 \times 1$ mm^3 were used for Seebeck coefficient (S) and electrical conductivity measurements in Waterloo. A commercial thermopower measurement apparatus (MMR Technologies) was used to measure S of various samples under dynamic vacuum

(16) *SAINT*, Version 4 ed.; Siemens Analytical X-ray Instruments Inc.: Madison, WI, 1995.
(17) Sheldrick, G. M. *SHELXTL*, Version 5.12 ed.; Siemens Analytical X-ray Systems: Madison, WI, 1995.
(18) Spek, A. L. *J. Appl. Crystallogr.* **2003**, *36*, 7−13.
(19) Andersen, O. K. *Phys. Rev. B* **1975**, *12*, 3060−3083.
(20) Skriver, H. L. *The LMTO Method;* Springer: Berlin, Germany, 1984.
(21) Hedin, L.; Lundqvist, B. I. *J. Phys. C* **1971**, *4*, 2064−2083.
(22) Lambrecht, W. R. L.; Andersen, O. K. *Phys. Rev. B* **1986**, *34*, 2439−2449.
(23) Blöchl, P. E.; Jepsen, O.; Andersen, O. K. *Phys. Rev. B* **1994**, *49*, 16223−16233.
(24) Dronskowski, R.; Blöchl, P. E. *J. Phys. Chem.* **1993**, *97*, 8617−8624.
(25) Landrum, G. A.; Dronskowski, R. *Angew. Chem., Int. Ed.* **2000**, *39*, 1560−1585.

Table 2. Atomic Coordinates, Equivalent Displacement Parameters, and Occupancy Factors[a] of $Ba_3Cu_{13.65}Te_{12}$

atom	site	x	y	z	U_{eq}/Å^2	occ.	occ.[a]
Ba1	4f	0.08425(4)	0.61146(3)	0.66459(5)	0.00842(11)	1	1
Ba2	4f	0.25204(4)	0.09850(2)	0.00295(5)	0.00862(11)	1	1
Ba3	4f	0.42668(5)	0.60730(3)	0.34199(5)	0.01045(11)	1	1
Te1	4f	0.08906(5)	0.15139(3)	0.16812(5)	0.00716(12)	1	1
Te2	4f	0.09596(5)	0.55948(3)	0.17001(6)	0.01076(12)	1	1
Te3	4f	0.10103(5)	0.06160(3)	0.66236(5)	0.00695(12)	1	1
Te4	4f	0.23661(5)	0.05968(3)	0.51383(5)	0.00746(12)	1	1
Te5	4f	0.24834(5)	0.66017(3)	0.49606(5)	0.00682(11)	1	1
Te6	4f	0.41588(5)	0.05920(3)	0.33261(5)	0.00819(12)	1	1
Te7	4f	0.58943(5)	0.05915(3)	0.14967(5)	0.00700(12)	1	1
Te8	4f	0.58938(5)	0.64840(3)	0.17032(5)	0.00615(11)	1	1
Te9	4f	0.73252(5)	0.06505(3)	0.00779(5)	0.00716(12)	1	1
Te10	2e	0.08554(7)	1/4	0.85001(8)	0.00599(15)	1	1
Te11	2e	0.08696(7)	1/4	0.49329(7)	0.00725(16)	1	1
Te12	2e	0.40824(7)	1/4	0.16132(8)	0.00626(15)	1	1
Te13	2e	0.41165(7)	1/4	0.50635(8)	0.00741(16)	1	1
Te14	2e	0.73691(7)	1/4	0.80972(8)	0.00655(16)	1	1
Te15	2e	0.75896(7)	1/4	0.19118(8)	0.00625(15)	1	1
Cu1	4f	0.03665(11)	0.65104(6)	0.27518(12)	0.0122(4)	0.926(5)	0.832(8)
Cu2	4f	0.06434(12)	0.67711(8)	0.06609(12)	0.0241(3)	1	1
Cu3	4f	0.14154(10)	0.54654(6)	0.40844(11)	0.0121(2)	1	1
Cu4	4f	0.16426(10)	0.18207(5)	0.70270(11)	0.0102(2)	1	1
Cu5	4f	0.1756(4)	0.0437(2)	0.2795(4)	0.0111(13)	0.265(5)	0.389(8)
Cu6	4f	0.25503(10)	0.68437(5)	0.00083(11)	0.0114(2)	1	1
Cu7	4f	0.33615(11)	0.17428(6)	0.31248(12)	0.0194(3)	1	0.923(9)
Cu8	4f	0.54239(11)	0.15095(6)	0.27732(11)	0.0140(2)	1	1
Cu9	4f	0.54832(10)	0.18216(6)	0.06807(11)	0.0113(2)	1	1
Cu10	4f	0.65470(10)	0.04669(6)	0.39376(11)	0.0125(2)	1	1
Cu11	4f	0.97060(11)	0.04135(6)	0.07732(13)	0.0152(4)	0.935(5)	0.756(8)
Cu12	2e	0.17306(14)	1/4	0.32700(15)	0.0115(3)	1	1
Cu13	2e	0.32782(13)	1/4	0.67341(15)	0.0104(3)	1	1
Cu14	2e	0.33426(14)	1/4	0.90593(15)	0.0096(3)	1	1
Cu15	2e	0.54737(13)	1/4	0.87442(16)	0.0112(3)	1	1
Cu16	2e	0.57570(14)	1/4	0.42036(16)	0.0121(3)	1	0.910(11)
Cu17	2e	0.92927(14)	1/4	0.58630(16)	0.0131(3)	1	1
Cu18	2e	0.94616(14)	1/4	0.12464(17)	0.0134(3)	1	1
Cu19	2e	0.164(5)	1/4	0.110(6)	0.04(2)	0.043(9)	0.148(11)

[a] Occupancy factors for $Ba_3Cu_{13.43(5)}Te_{12}$.

in the temperature range between 300 and 550 K, using constantan as an internal standard to determine the temperature difference. Silver paint (TED PELLA) was used to create the electric contacts. The specific electrical conductivities (σ) were (indirectly) measured using a four-point method in each case at the same bar that was used for the Seebeck coefficient determinations. A self-made device was used to determine the voltage drops ΔV over distances (L) of approximately 2 mm at currents between 0.2 and 0.6 mA under dynamic vacuum between 300 and 180 K. The achieved densities were between 75% and 80% of the theoretical maximum determined via the single-crystal structure studies. The resistances (R) were calculated from the voltage drops using Ohm's law, i.e., $R = \Delta V/I$, with $I =$ current. σ(T) was calculated after measuring the lengths between the contacts, L, according to $\sigma = L/(AR)$, with the area $A = 1\text{ mm} \times 1\text{ mm}$.

The properties of the sample of the nominal composition $Ba_3Cu_{13.88}Te_{12}$ were determined in Clemson. There, the electrical resistivity and thermopower were measured concurrently over a temperature range of about 10−328 K using a custom-designed apparatus that has been described previously.[26] Resistivity was measured using the standard four-probe technique and the direction of current is reversed to subtract off any thermal voltages. The thermopower was calculated by the ratio of the thermoelectric voltage to the temperature gradient while zero current was injected.

Thermal conductivity was measured using the steady-state technique from 10 to 325 K using a custom-designed sample puck that plugs into the coldfinger of a closed cycle refrigerator.[27] The sample was mounted on a stable temperature copper base, with two #38 Cu wires attached to the sample using Stycast epoxy resin, onto which a 1-mil Cn-Cromega-Cn thermocouple is attached. A 120-Ω strain gauge is attached on the top of the sample with a thin layer of epoxy to provide heating power ($P = I^2R$). The heater current is determined by measuring the voltage across a standard resistor in series with the heater. The resulting temperature gradient (ΔT) is measured using the thermocouple. The base temperature is held to within ±20 mK over the entire measurement sequence. All the various measurement techniques for the electrical and thermal transport properties are discussed in intricate detail in a recent review article.[28]

Results and Discussion

Crystal Structure. The structure of $Ba_3Cu_{14-\delta}Te_{12}$ is shown in Figure 1, which emphasizes the Cu−Te contacts. This is a very complex three-dimensional structure, with all lattice parameters being >11.9 Å. Each Cu atom is surrounded by three or four Te neighbors and each Ba atom by nine Te atoms in form of distorted monocapped square antiprisms. The coordination of the Ba atoms is typical for ternary barium tellurides, both with respect to the coordination polyhedra and the Ba−Te distances of 3.47−3.84 Å

(26) Pope, A. L.; Littleton, R. T., IV; Tritt, T. M. *Rev. Sci. Instrum.* **2001**, *72*, 3129−3131.

(27) Pope, A. L.; Zawilski, B.; Tritt, T. M. *Cryogenics* **2001**, *41*, 725−731.

(28) Tritt, T. M. In *CRC Handbook on Thermoelectrics*; Rowe, D. M., Ed.; CRC Press: Boca Raton, FL, 2005.

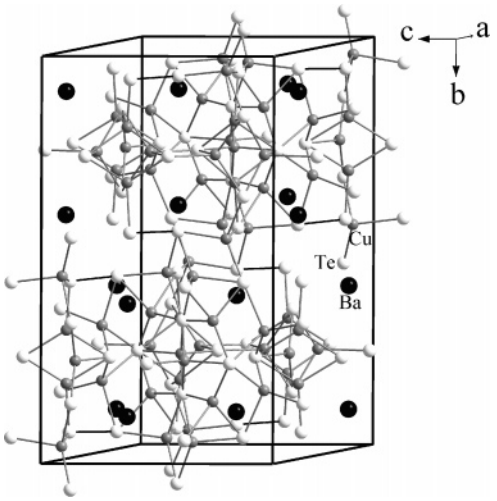

Figure 1. Crystal structure of $Ba_3Cu_{14-\delta}Te_{12}$. Black circles, Ba; gray, Cu; white, Te. Ba−Te bonds are omitted for clarity, and Te−Te bonds are emphasized via black lines.

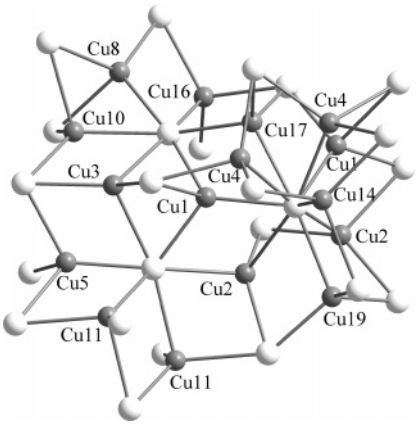

Figure 2. A section of the covalent Cu−Te network of $Ba_3Cu_{14-\delta}Te_{12}$. Gray, Cu; white, Te.

(Table 3). Examples include $BaSbTe_3$ (nine Ba−Te bonds per Ba atom between 3.41 and 3.89 Å)[29] and Ba_2SnTe_5 (again nine bonds, 3.44−3.84 Å).[12]

A section of the three-dimensionally extended Cu−Te network is depicted in Figure 2. The dominating motifs therein are the (distorted) $CuTe_4$ tetrahedra, which are interconnected via all three common possibilities, i.e., by corner-, edge-, and face-sharing. For example, the Cu1 centered tetrahedron shares a face with the Cu3, an edge with the Cu4, and a corner with the next Cu1 tetrahedron. The Cu−Te bonds between 2.50 and 2.85 Å are indicative of Cu^+, as a comparison with $(Ba^{2+})(Cu^+)_2(Te^{2-})_2$ with its Cu−Te distances of 2.59−2.81 Å[14] reveals.

This includes the Cu19 site with its Cu−Te bonds between 2.50 and 2.81 Å, which shows an occupancy of only 4% in the case of $Ba_3Cu_{13.65}Te_{12}$ ($Ba_3Cu_{13.43}Te_{12}$: 15%). The coordination spheres of the other Cu sites with significant deficiencies (Cu1, Cu5, Cu7, Cu11, and Cu16) are inconspicuous as well. It is noted that Cu deficiencies are often observed in copper tellurides, e.g. occurring in $Cu_{2-\delta}Te$[30] and $TlCu_{2-\delta}Te_2$.[31]

Table 3. Selected Interatomic Distances [Å] of $Ba_3Cu_{13.65}Te_{12}$

Ba1−Te15	3.4845(8)	Ba2−Te9	3.4736(10)	Ba3−Te8	3.5172(9)
Ba1−Te5	3.5429(9)	Ba2−Te1	3.5263(9)	Ba3−Te6	3.5278(10)
Ba1−Te1	3.5720(9)	Ba2−Te8	3.5444(9)	Ba3−Te5	3.5696(9)
Ba1−Te11	3.5821(8)	Ba2−Te6	3.6177(9)	Ba3−Te13	3.5993(8)
Ba1−Te4	3.5970(9)	Ba2−Te7	3.6742(9)	Ba3−Te14	3.6065(8)
Ba1−Te9	3.6526(9)	Ba2−Te3	3.7176(10)	Ba3−Te6	3.6197(9)
Ba1−Te7	3.6620(9)	Ba2−Te12	3.7602(10)	Ba3−Te2	3.6602(9)
Ba1−Te3	3.6693(9)	Ba2−Te10	3.7780(10)	Ba3−Te4	3.7115(9)
Ba1−Te3	3.6706(10)	Ba2−Te2	3.7863(10)	Ba3−Te9	3.8378(10)
Cu1−Te2	2.5799(15)	Cu2−Te14	2.6160(14)	Cu3−Te4	2.5757(13)
Cu1−Te10	2.6023(13)	Cu2−Te14	2.6444(14)	Cu3−Te3	2.6336(13)
Cu1−Te5	2.7065(13)	Cu2−Te2	2.7331(17)	Cu3−Te5	2.7007(13)
Cu1−Te3	2.8200(15)	Cu2−Te10	2.8657(17)	Cu3−Cu10	2.5043(16)
Cu1−Cu17	2.5880(17)	Cu2−Cu18	2.713(2)	Cu3−Cu5	2.602(5)
Cu1−Cu4	2.6084(17)	Cu2−Cu6	2.7219(18)		
Cu1−Cu3	2.6815(17)	Cu2−Cu19	3.00(5)	Cu6−Te9	2.5358(13)
Cu1−Cu2	2.7282(19)			Cu6−Te14	2.6259(14)
		Cu5−Te2	2.502(4)	Cu6−Te15	2.6274(14)
Cu4−Te3	2.6414(14)	Cu5−Te4	2.582(5)	Cu6−Cu15	2.5498(16)
Cu4−Te11	2.6665(14)	Cu5−Te1	2.607(4)	Cu6−Cu18	2.5794(17)
Cu4−Te8	2.7145(12)	Cu5−Te6	2.654(4)	Cu6−Cu6	2.779(2)
Cu4−Te10	2.7513(14	Cu5−Cu11	2.540(4)	Cu6−Cu9	2.8156(16)
Cu4−Cu13	2.5707(17)				
Cu4−Cu14	2.7587(17)	Cu7−Te6	2.5862(15)	Cu8−Te12	2.6196(13)
Cu4−Cu4	2.877(2)	Cu7−Te13	2.6220(15)	Cu8−Te7	2.6855(14)
Cu4−Cu17	2.8797(17)	Cu7−Te1	2.6931(13)	Cu8−Te6	2.7187(14)
		Cu7−Te12	2.8292(17)	Cu8−Te5	2.7319(13)
Cu9−Te8	2.6640(13)	Cu7−Cu12	2.5848(17)	Cu8−Cu16	2.6220(16)
Cu9−Te15	2.6766(13)	Cu7−Cu8	2.7196(18)	Cu8−Cu9	2.6249(18)
Cu9−Te7	2.7468(14)	Cu7−Cu19	2.85(5)	Cu8−Cu10	2.6288(17)
Cu9−Te12	2.7913(14)	Cu7−Cu16	3.0040(18)		
Cu9−Cu15	2.725(2)			Cu11−Te2	2.5517(14)
Cu9−Cu14	2.7979(17)	Cu10−Te4	2.5826(13)	Cu11−Te9	2.6144(13)
Cu9−Cu9	2.873(2)	Cu10−Te6	2.6076(12)	Cu11−Te1	2.6845(15)
		Cu10−Te7	2.6757(14)	Cu11−Te2	2.7241(16)
Cu12−Te11	2.6232(19)	Cu10−Te5	2.7318(14)	Cu11−Cu11	2.858(3)
Cu12−Te13	2.6710(16)				
Cu12−Te1	2.6928(12)	Cu13−Te13	2.6121(19)	Cu14−Te8	2.6545(12)
Cu12−Te1	2.6928(12)	Cu13−Te11	2.6927(16)	Cu14−Te8	2.6545(12)
Cu12−Cu19	2.56(6)	Cu13−Te8	2.7252(12)	Cu14−Te10	2.7233(17)
Cu12−Cu18	2.687(2)	Cu13−Te8	2.7252(12)	Cu14−Te12	2.7726(19)
		Cu13−Cu15	2.628(2)	Cu14−Cu15	2.731(2)
Cu15−Te8	2.6026(10)	Cu13−Cu14	2.752(2)		
Cu15−Te8	2.6026(10)			Cu17−Te11	2.5834(19)
Cu15−Te14	2.6998(18)	Cu16−Te13	2.5905(18)	Cu17−Te5	2.6768(12)
		Cu16−Te5	2.6649(12)	Cu17−Te5	2.6768(12)
Cu18−Te1	2.5923(11)	Cu16−Te5	2.6649(12)	Cu17−Te10	2.8454(19)
Cu18−Te1	2.5923(11)	Cu16−Te12	2.8245(19)		
Cu18−Te15	2.6876(19)			Cu19−Te1	2.50(3)
Cu18−Cu19	2.69(4)	Te3−Te4	2.8968(9)	Cu19−Te1	2.50(3)
		Te7−Te9	2.9064(9)	Cu19−Te12	2.68(4)
				Cu19−Te10	2.81(7)

In addition to the $CuTe_4$ units, three crystallographically independent triangular-shaped $CuTe_3$ units are present in the structure of $Ba_3Cu_{14-\delta}Te_{12}$, with Cu6, Cu15, and Cu18 as the central atoms. While the 3-fold coordination is less common for Cu atoms, it is not extremely unusual, for example, also occurring in $Ba_3Cu_2Sn_3Se_{10}$. The interconnection of the $CuTe_3$ units is shown in Figure 3, with a mirror plane going through Cu15, Te14, Te15, and Cu18. The four Cu atoms therein form a planar rhomb with Cu−Cu distances between 2.55 and 2.78 Å.

Moreover, two Te_2 dumbbells are bonded to the Cu_4 cluster of Figure 3, with Te−Te bonds of 2.90 and 2.91 Å. $Ba_3Cu_{14}Te_{12}$ is a polytelluride with two Te_2^{2-} units per formula unit, thus according to the formulation $(Ba^{2+})_3(Cu^+)_{14}(Te_2^{2-})_2(Te^{2-})_8$, an electron-precise material.

The numerous Cu−Cu interactions <3 Å are extended along all three dimensions of the crystal structure. Chains

(29) Volk, K.; Cordier, G.; Cook, R.; Schäfer, H. *Z. Naturforsch. B* **1980**, *35*, 136−140.
(30) Sridhar, K.; Chattopadhyay, K. *J. Alloys Compd.* **1998**, *264*, 293−298.
(31) Ohtani, T.; Taniguchi, M.; Sasaki, S.; Kishi, H.; Nakata, T. *J. Alloys Compd.* **2004**, *383*, 245−250.

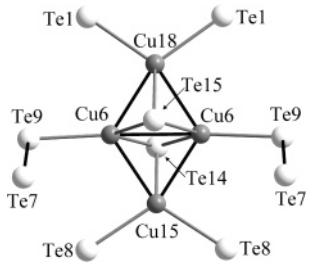

Figure 3. Connection of the $CuTe_3$ units with the Te_2^{2-} dumbbells of $Ba_3Cu_{14-\delta}Te_{12}$. Gray, Cu; white, Te.

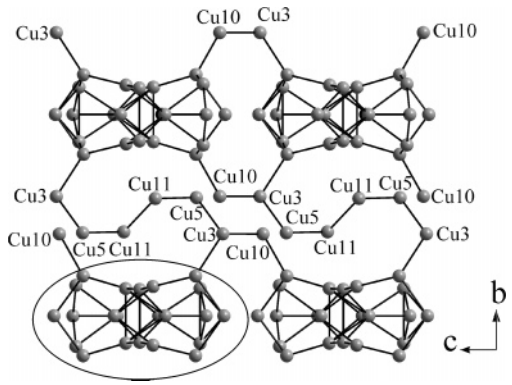

Figure 4. Three-dimensional network of Cu−Cu interactions of $Ba_3Cu_{14-\delta}Te_{12}$.

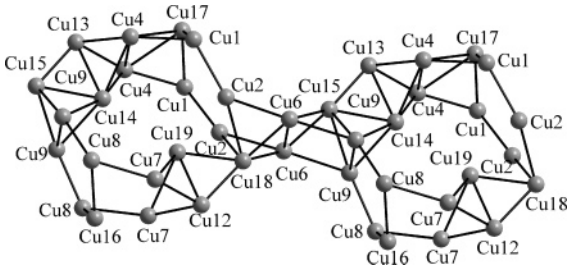

Figure 5. Two Cu_{20} rings interconnected via two Cu6 atoms (circled area of Figure 4). Horizontal: *a* axis.

of Cu atoms (Cu10, Cu3, and Cu5) connect a large "cluster"—circled in Figure 4—both along the *b* axis as well as along the *c* axis.

The "cluster" is composed of rings each comprising 20 Cu atoms, interconnected via $Cu6_2$ bridges along the *a* axis (Figure 5). The occurrence of Cu−Cu interactions <3 Å is typical for CuI compounds,[32] and such interactions were also found in the binary copper tellurides $Cu_{2-\delta}Te$[30] and Cu_7Te_4.[33] Moreover, Cu−Cu bonds were identified in $BaCu_2Te_2$[14] as well.

Electronic Structure. The densities of states of the *$Ba_3Cu_{14}Te_{12}$* model (left part of Figure 6) reveal a small band gap of 0.1 eV directly at the Fermi level, E_F, which was arbitrarily placed at 0 eV. The existence of a gap confirms the validity of the electron-precise formulation $(Ba^{2+})_3(Cu^+)_{14}(Te_2^{2-})_2(Te^{2-})_8$. The large valence band is extended over more than 7 eV and is mostly comprised of Te-p and Cu-d states. The latter dominate the region between −2.5 and −4 eV. The small size of the band gap is related to the existence of empty, strongly antibonding Te−Te states of the Te_2^{2-} units commencing at +0.1 eV. Neither the Cu−Cu nor the

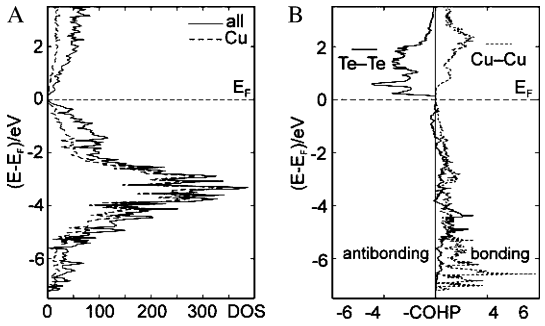

Figure 6. Densities of states (DOS, A) and cumulated Cu−Cu and Te−Te crystal orbital Hamilton populations (COHP, B) of the model *$Ba_3Cu_{14}Te_{12}$*.

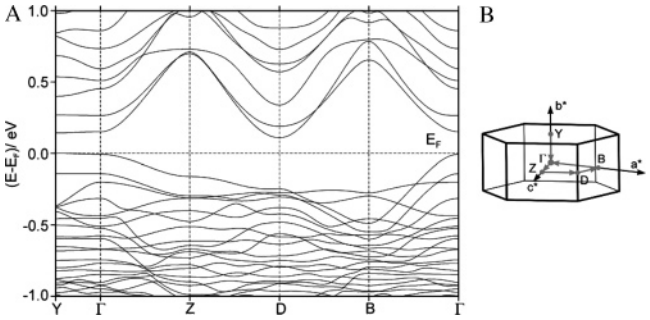

Figure 7. Band structure (A) of the model *$Ba_3Cu_{14}Te_{12}$* and the corresponding Brillouin zone (B).

Cu−Te interactions show significant contributions directly above E_F. In contrast to the Te−Te interactions, the Cu−Cu bonds continue to exhibit bonding states above E_F (right part of Figure 6).

Overall, these Te−Te interactions around 2.9 Å are quite strong, with mostly bonding states filled, and integrated COHP values (ICHOP) between −1.28 and −1.42 eV/bond (strong interactions are reflected in large negative values). For comparison, the Te−Te bonds of Ba_2SnTe_5 exhibit ICOHP values between −1.98 and −0.81 eV/bond.[12] The strongest Cu−Cu interactions of *$Ba_3Cu_{14}Te_{12}$* have ICOHP values above −0.9 eV/bond, larger than those in $BaCu_2SnSe_4$ (−0.32 eV for the 2.70 Å interaction) and in $Ba_3Cu_2Sn_3Se_{10}$ (−0.75 eV, 2.65 Å).[13]

The band structure of the *$Ba_3Cu_{14}Te_{12}$* model is shown in Figure 7, with the inset depicting the first Brillouin zone. The special points were selected according to the Bradley/Cracknell conventions.[34] Both the highest filled and the lowest empty band have regions with extremely flat slopes (between Y and Γ, i.e., along *b**) as well as steep slopes (e.g., between B and Γ, i.e., along *a**). The slope of the lowest conduction band is directly related to the Te_2^{2-} dumbbells lying perpendicular to the *b* axis (Figure 1). The steep slope is indicative of fast charge carriers, and the flat slope corresponds to high effective masses, pointing toward the possibility of high Seebeck coefficients, if $\delta = 0$ could be achieved in $Ba_3Cu_{14-\delta}Te_{12}$.

Physical Properties. The experimentally determined Seebeck coefficients (*S*) of $Ba_3Cu_{14-\delta}Te_{12}$ are shown for $\delta =$ 0.025, 0.5, 0.675, and 0.825 in the left part of Figure 8. The values of *S* range from +36 to +53 μV/K at 300 K and from +72 to +108 μV/K at 545 K. No clear dependence on

(32) Pyykkö, P. *Chem. Rev.* **1997**, *97*, 597−636.
(33) Matar, S. F.; Weihrich, R.; Kurowski, D.; Pfitzner, A. *Solid State Sci.* **2004**, *6*, 15−20.
(34) Bradley, C. J.; Cracknell, A. P. *The Mathematical Theory of Symmetry in Solids*; Clarendon Press: Oxford, 1972.

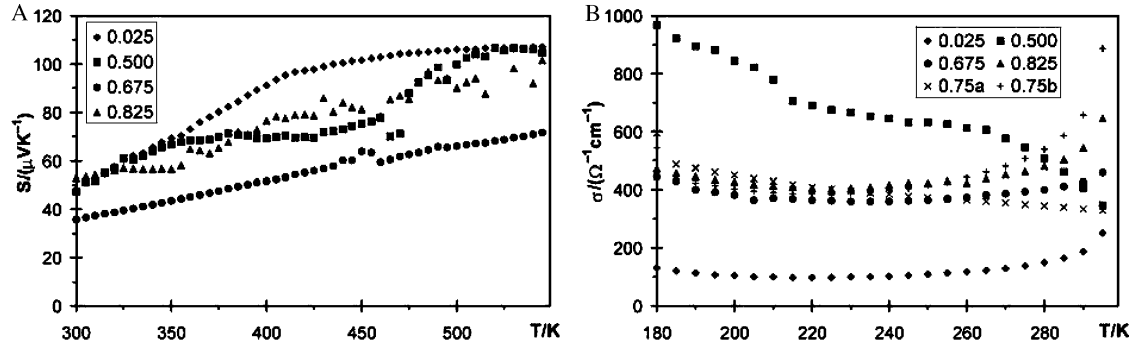

Figure 8. Seebeck coefficients (A) and electrical conductivities (B) of $Ba_3Cu_{14-\delta}Te_{12}$.

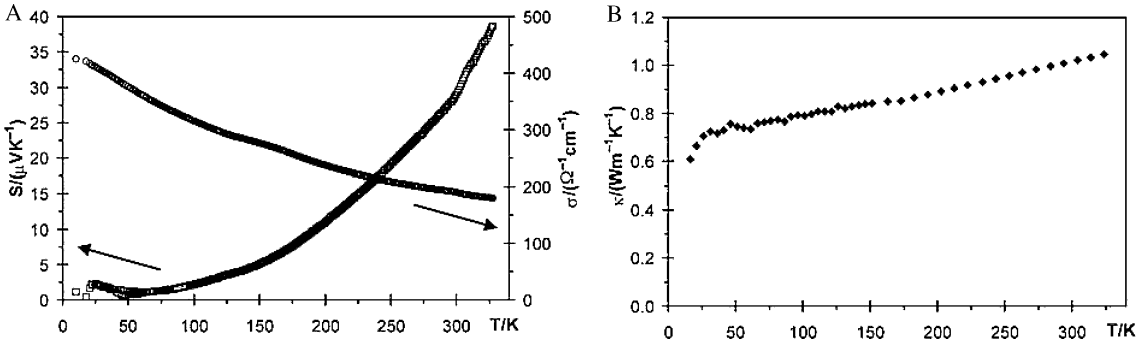

Figure 9. (A) Seebeck coefficients (squares) and electrical conductivities (circles) of $Ba_3Cu_{13.88}Te_{12}$. (B) Thermal conductivities of $Ba_3Cu_{13.88}Te_{12}$.

δ was found. The range is typical for a degenerate p-type semiconductor, consistent with the electronic structure calculations, suggesting an intrinsic semiconductor for $\delta = 0$; for $\delta > 0$, the dominating charge carriers should be p-type. It is noted that all attempts to prepare phase-pure $Ba_3Cu_{14-\delta}Te_{12}$ with $\delta = 0$ resulted in mixtures of $Ba_3Cu_{14-\delta}Te_{12}$ and $Cu_{2-\delta}Te$.

The same range of samples ($0.025 \leq \delta \leq 0.825$) was subjected to electrical conductivity (σ) measurements (right part of Figure 8). The absolute values of σ are between 100 and 1000 Ω^{-1} cm^{-1}. The temperature trend is mostly but not strictly negative; that is, increasing temperature occurs with decreasing electrical conductivities. While the pellet with the smallest δ value of 0.025 exhibits the smallest conductivity, there is no definite dependence on δ.

The Seebeck coefficient and electrical conductivity were simultaneously determined on a sample of the nominal composition $Ba_3Cu_{14-\delta}Te_{12}$ (i.e., $\delta = 0.12$) between 10 and 328 K. This sample exhibits qualitatively the same trends, i.e., the Seebeck coefficient increased and the electrical conductivity decreased with increasing temperature (left part of Figure 9). This manifests these qualitative trends between 10 and 550 K for the Seebeck coefficients and between 10 and 325 K for the electrical conductivity. Moreover, the 300 K values of the sample with $\delta = 0.12$ as measured at Clemson are comparable, with $S = +30$ μV/K and $\sigma = 190$ Ω^{-1} cm^{-1}, indicating that both (a) the $\delta = 0.12$ composition is not special and (b) the different measurement methods applied in Waterloo and Clemson, respectively, yield comparable results.

The thermal conductivity (κ) of the sample of the nominal composition $Ba_3Cu_{13.88}Te_{12}$ was measured between 16 and 324 K (right part of Figure 9). Starting at 65 K, κ increases linearly with increasing temperature, to the extremely small value of 1.08 W m^{-1} K^{-1} at 300 K. This is even lower than those in the recently characterized $Cs_2BaCu_8Te_{10}$ (1.2 W m^{-1} K^{-1}) and $Rb_2BaCu_8Te_{10}$ (1.4 W m^{-1} K^{-1}) that were appropriately described as materials with "very low thermal conductivity".[15] The electrical contribution, κ_{el}, to the overall thermal conductivity $Ba_3Cu_{13.88}Te_{12}$ at 300 K is estimated to be 0.14 W m^{-1} K^{-1}, according to the Wiedemann−Franz law $\kappa_{el} = L\sigma T$, with the Lorentz number $L = 2.45 \times 10^{-8}$ WΩ/K^2,[35] and $\sigma = 190$ Ω^{-1} cm^{-1}. This leaves the lattice contribution, κ_L, at $\kappa_L = \kappa - \kappa_{el} = 0.94$ W m^{-1} K^{-1}. Overall, the thermal conductivity is lower than those in most commercial thermoelectric materials, likely a consequence of the low symmetry of $Ba_3Cu_{14-\delta}Te_{12}$ and the significant Cu disorder.

The (dimensionless) thermoelectric *figure-of-merit*, $ZT = TS^2\sigma/\kappa$, of $Ba_3Cu_{14}Te_{12}$ increases from 0.001 at 200 K to 0.007 at 320 K, while advanced thermoelectrics may exhibit or even exceed $ZT = 1$. A comparison with these leading thermoelectric materials reveals that the thermal conductivity is more than competitive, but the Seebeck coefficients should be at least 100 μV/K. For example, optimized $CsBi_4Te_6$ doped with 0.05% SbI_3 exhibits $S = +175$ μV/K, $\sigma = 1800$ Ω^{-1} cm^{-1}, and $\kappa = 1.55$ W m^{-1} K^{-1} at its optimal temperature of 225 K; thus, $ZT = 0.8$.[9] The filled skutterudite $LaFe_3CoSb_{12}$ exhibits $S = +104$ μV/K, $\sigma = 630$ Ω^{-1} cm^{-1}, and $\kappa = 1.6$ W m^{-1} K^{-1} at 300 K; thus, $ZT = 0.13$, with an estimated $ZT = 1.4$ at 1000 K (values extracted from the published figures).[5]

Because of its extremely low thermal conductivity, a study of precisely doped $Ba_3Cu_{14}Te_{12}$ would be very interesting, with only one kind of charge carriers remaining. To this end,

(35) Kittel, C. *Introduction to Solid State Physics*, 7th ed.; John Wiley & Sons: New York, 1996.

we are investigating partial substitutions of Ba with La and of Cu with Ag.

Acknowledgment. Financial support from NSERC, CFI, OIT (Ontario Distinguished Researcher Award for H.K.), the Province of Ontario (Premier's Research Excellence Award for H.K.), and the Canada Research Chair program (CRC for H.K.) is appreciated. We acknowledge the financial support of the Department of Energy for DOE Implementation Grant (DOE#: DE: FG02-04ER-46139) and the financial support of the Office of Naval Research for DEPSCoR Grant #N00014-0310787.

Supporting Information Available: Two X-ray crystallographic files in CIF format.

CM060776K